DNA DAMAGE

Coupled Activation and Degradation of eEF2K Regulates Protein Synthesis in Response to Genotoxic Stress

Flore Kruiswijk,[1] Laurensia Yuniati,[1] Roberto Magliozzi,[1] Teck Yew Low,[2,3] Ratna Lim,[1] Renske Bolder,[1] Shabaz Mohammed,[2,3] Christopher G. Proud,[4] Albert J. R. Heck,[2,3] Michele Pagano,[5,6] Daniele Guardavaccaro[1]*

The kinase eEF2K [eukaryotic elongation factor 2 (eEF2) kinase] controls the rate of peptide chain elongation by phosphorylating eEF2, the protein that mediates the movement of the ribosome along the mRNA by promoting translocation of the transfer RNA from the A to the P site in the ribosome. eEF2K-mediated phosphorylation of eEF2 on threonine 56 (Thr^{56}) decreases its affinity for the ribosome, thereby inhibiting elongation. Here, we show that in response to genotoxic stress, eEF2K was activated by AMPK (adenosine monophosphate–activated protein kinase)–mediated phosphorylation on serine 398. Activated eEF2K phosphorylated eEF2 and induced a temporary ribosomal slowdown at the stage of elongation. Subsequently, during DNA damage checkpoint silencing, a process required to allow cell cycle reentry, eEF2K was degraded by the ubiquitin-proteasome system through the ubiquitin ligase $SCF^{\beta TrCP}$ (Skp1–Cul1–F-box protein, β-transducin repeat–containing protein) to enable rapid resumption of translation elongation. This event required autophosphorylation of eEF2K on a canonical βTrCP-binding domain. The inability to degrade eEF2K during checkpoint silencing caused sustained phosphorylation of eEF2 on Thr^{56} and delayed the resumption of translation elongation. Our study therefore establishes a link between DNA damage signaling and translation elongation.

INTRODUCTION

Cells activate surveillance molecular networks known as DNA damage checkpoints to protect their genome from environmental and metabolic genotoxic stress. Depending on the type and extent of DNA lesions and the cellular context, damaged cells with an activated checkpoint can undergo senescence, die by apoptotic cell death, or repair the damaged genome and, after checkpoint termination, resume their physiological functions (*1*, *2*).

Genotoxic stress has a greater effect on gene expression at the level of mRNA translation than at the level of transcription (*3*). This may be due to the fact that protein synthesis requires about 40% of the total cellular energy, and cells need to couple stress responses to metabolic demands (*4*). Indeed, it is conceivable that in response to genotoxic stress, cells aim to preserve energy by reducing protein synthesis to be able to repair the damage.

The mTOR (mammalian target of rapamycin) pathway integrates growth and stress signals and promotes protein synthesis. mTOR regulates several critical components involved in both translation initiation and elongation. mTOR-mediated phosphorylation of two proteins that promote translation initiation, the p70 ribosomal S6 kinase (S6K) and eukaryotic initiation factor 4E (eIF4E) binding protein 1 (4E-BP1), increases their activity (*5*, *6*). In addition, mTOR promotes translation elongation by inhibiting eukaryotic elongation factor 2 (eEF2) kinase (eEF2K), which phosphorylates and inactivates eEF2, a factor that mediates the translocation step of peptide-chain elongation (*7*–*13*). eEF2K-mediated phosphorylation of eEF2 on Thr^{56} reduces the affinity of eEF2 for the ribosome, thereby inhibiting its function (*13*–*23*). The activity of eEF2K is controlled under various conditions. For example, stimuli that induce protein synthesis trigger the inactivation of eEF2K and the subsequent dephosphorylation of eEF2 (*24*). In contrast, deficiencies in nutrients or energy lead to activation of eEF2K and impairment of translation elongation.

Despite the major impact of genotoxic stress on mRNA translation, no information is available on how translation elongation is affected by genotoxic stress, and, more generally, there have been few studies directed to understanding the regulation of protein synthesis by the DNA damage response. DNA damage inhibits the mTOR-S6K axis through p53, a key sensor of genotoxic stress, thereby leading to decreased protein synthesis (*25*, *26*). Moreover, the activity of TSC2 (tuberous sclerosis 2), a crucial inhibitor of mTOR, has been reported to be induced by p53 (*26*).

Numerous studies have uncovered fundamental functions of the ubiquitin-proteasome system in the DNA damage response (*1*, *2*, *27*). This system involves two discrete and sequential processes: the tagging of substrates by covalent attachment of multiple ubiquitin molecules and the degradation of polyubiquitylated proteins by the 26*S* proteasome (*28*). Ubiquitin is transferred and covalently attached to substrates through an enzymatic cascade involving ubiquitin-activating enzymes (E1), ubiquitin-conjugating enzymes (E2), and ubiquitin ligases (E3). E3 ubiquitin ligases represent the essential regulators of ubiquitylation because they physically interact with target substrates, linking them to E2 ubiquitin-conjugating enzymes.

[1]Hubrecht Institute–KNAW and University Medical Center Utrecht, Uppsalalaan 8, 3584 CT Utrecht, Netherlands. [2]Biomolecular Mass Spectrometry and Proteomics, Bijvoet Center for Biomolecular Research and Utrecht Institute for Pharmaceutical Sciences, Utrecht University, Padualaan 8, 3584 CH Utrecht, Netherlands. [3]Netherlands Proteomics Center, Padualaan 8, 3584 CH Utrecht, Netherlands. [4]School of Biological Sciences, School of Biological Sciences, Life Sciences Building, University of Southampton, Southampton SO17 1BJ, UK. [5]Department of Pathology, NYU Cancer Institute, New York University School of Medicine, 522 First Avenue, SRB1107, New York, NY 10016, USA. [6]Howard Hughes Medical Institute.
*To whom correspondence should be addressed. E-mail: d.guardavaccaro@hubrecht.eu

$SCF^{\beta TrCP}$ (Skp1–Cul1–F-box protein, β-transducin repeat–containing protein) is a multisubunit RING finger–type ubiquitin ligase composed of a cullin scaffold, Cul1, which simultaneously interacts with the RING subunit Rbx1 and the adaptor protein Skp1 (*29*–*32*). Skp1 in turn binds the F-box protein βTrCP, the substrate receptor subunit that recruits specific substrate proteins. Through its WD40 β-propeller structure, βTrCP recognizes a diphosphorylated motif with the consensus DpSGXX(X)pS in which the serine residues are phosphorylated to allow interaction with βTrCP.

Here, we show that upon genotoxic stress, eEF2K is first activated by AMPK (adenosine monophosphate–activated protein kinase)–mediated phosphorylation to induce a temporary translational slowdown at the stage of elongation and then, during checkpoint silencing, is targeted for proteasome-dependent degradation by the ubiquitin ligase $SCF^{\beta TrCP}$ to allow rapid and efficient resumption of translation. These findings establish an important link between DNA damage response and translation of mRNAs.

RESULTS

eEF2K specifically interacts with βTrCP1 and βTrCP2

To identify substrates of the ubiquitin ligase $SCF^{\beta TrCP}$, we used immunoaffinity chromatography followed by tandem mass spectrometry (MS/MS). We expressed FLAG–hemagglutinin (HA) epitope–tagged βTrCP2 (FLAG-HA-βTrCP2) in human embryonic kidney (HEK) 293T cells and analyzed by MS proteins that co-purified with FLAG-HA-βTrCP2 after sequential FLAG and HA immunoprecipitations. We unambiguously identified eEF2K, recording 26 spectra corresponding to nine unique peptides (fig. S1A). To validate the interaction between βTrCP and eEF2K, we examined the ability of FLAG-tagged versions of 29 F-box proteins expressed in HEK293T cells to bind to endogenous eEF2K. βTrCP1 and βTrCP2 were the only F-box proteins that interacted with eEF2K (Fig. 1A and fig. S1B). βTrCP1 and βTrCP2 share identical biochemical properties and substrates; hence, the term βTrCP will refer to both unless specified otherwise. The βTrCP-eEF2K interaction was detected in other cell types and thus was not restricted to HEK293T cells (fig. S1C). Moreover, when we followed the reciprocal approach and immunopurified eEF2K expressed in HEK293T cells, we recovered peptides corresponding to βTrCP1 (one unique peptide), βTrCP2 (four unique peptides), and the SCF adaptor Skp1 (one unique peptide) (fig. S1, D to F). The ability of eEF2K to immunoprecipitate the βTrCP1-Skp1 complex was confirmed by immunoprecipitation followed by immunoblotting (Fig. 1B). The interaction of endogenous βTrCP1 and eEF2K was also observed (Fig. 1C).

To obtain insight into the nature of the βTrCP-eEF2K interaction, we mutated the arginine residue (Arg^{474} of human βTrCP1, isoform 2) in the WD40 β-propeller structure of βTrCP1 that interacts with the substrate destruction motif (*32*) and analyzed its ability to bind eEF2K. Whereas wild-type βTrCP1 immunoprecipitated eEF2K and the established βTrCP1 substrate PDCD4, the βTrCP1(R474A) mutant did not (Fig. 1D, left panels). Similar results were obtained when we mutated the equivalent arginine residue in βTrCP2 (Arg^{447} of human βTrCP2, isoform C; Fig. 1D, right panels).

eEF2K interaction with βTrCP requires a conserved phosphodegron

The WD40 β-propeller structure of βTrCP binds its substrates through a diphosphorylated degradation motif (phosphodegron) with the consensus DpSGXX(X)pS (*30*–*32*), but some substrates of βTrCP have one or both serine residues replaced by either aspartic acid or glutamic acid (*33*–*35*). eEF2K has four of these potential βTrCP-binding domains (Fig. 2A, top). To identify the domain required for the interaction with βTrCP, we generated various serine–, aspartic acid–, or glutamic acid–to–alanine double mutants and examined their ability to bind βTrCP. The eEF2K(S441A/S445A) mutant immunoprecipitated less βTrCP1 compared to wild-type eEF2K, eEF2K(S71A/S78A), eEF2K(S72A/S78A), eEF2K(S622A/S627A), or eEF2K(E652A/D657A) (Fig. 2A, bottom). The motif surrounding Ser^{441} and Ser^{445} is highly conserved in vertebrate orthologs of eEF2K (Fig. 2B).

Next, we used MS to analyze phosphorylation of eEF2K in this region (*36*). FLAG epitope–tagged eEF2K was coexpressed with a Cul1 dominant-negative deletion mutant [Cul1-N252 (*37*)] in HEK293T cells and immunopurified. Analysis of the recovered eEF2K phosphopeptides demonstrated that Ser^{441} and Ser^{445} were phosphorylated in cells (fig. S2). To test whether phosphorylation is required for the interaction of eEF2K with βTrCP, we used immobilized synthetic peptides that make up the βTrCP-binding domain of eEF2K (amino acids 438 to 450 in human eEF2K). Although an eEF2K peptide containing phosphorylated Ser^{441} and Ser^{445} interacted with βTrCP1 (but not with FBXW5), the corresponding nonphosphorylated peptide was unable to do so (Fig. 2C), indicating that phosphorylation of Ser^{441} and Ser^{445} was required for the association with βTrCP.

To test whether $SCF^{\beta TrCP}$ was directly responsible for the polyubiquitylation of eEF2K, we reconstituted the ubiquitylation of eEF2K in vitro. Immunopurified βTrCP1, but not an inactive βTrCP1(ΔF-box) mutant, induced the in vitro ubiquitylation of eEF2K (Fig. 2D). Moreover, the eEF2K(S441A/S445A) mutant was not efficiently ubiquitylated by βTrCP in vitro (fig. S3). Thus, consistently with our findings in cultured cells, the in vitro data show that βTrCP promotes the ubiquitylation of eEF2K in a phosphodegron-dependent manner.

eEF2K is degraded during silencing of the G_2 DNA damage checkpoint

Because mRNA translation is regulated by mitogens, we analyzed their effect on the abundance of eEF2K. We serum-starved T98G cells (revertants from T98 glioblastoma cells that acquired the property to accumulate in G_0-G_1 after serum deprivation) for 72 hours and then reactivated them by adding serum. We observed a slight decrease in the abundance of eEF2K in response to mitogens (fig. S4A). However, this decrease is not mediated by $SCF^{\beta TrCP}$ because eEF2K abundance was not affected when we silenced βTrCP by transfecting T98G cells with a double-stranded RNA oligonucleotide that efficiently silenced both βTrCP1 and βTrCP2 (fig. S4A) (*33*, *38*–*41*).

Because eEF2K is a crucial inhibitor of translation elongation and because inhibition of protein synthesis is a common response to stress conditions (*8*, *10*, *23*, *42*, *43*), we analyzed the abundance of eEF2K in response to hypoxic and genotoxic stress. Hypoxia (and recovery from it) did not appear to result in detectable changes in the abundance of eEF2K (fig. S4B). Next, we examined eEF2K abundance in response to genotoxic stress. U2OS cells were synchronized in the G_2 phase of the cell cycle and then treated with a low dose of doxorubicin to activate the G_2 DNA damage checkpoint. Subsequently, cells were allowed to recover from the DNA damage checkpoint after extensive washing in drug-free medium. The abundance of eEF2K steadily decreased during checkpoint silencing, paralleling the decrease in the phosphorylation of Chk2 at Thr^{68} and that of histone 2AX at Ser^{139} (Fig. 3A). A similar pattern of changes in eEF2K abundance was observed in experiments in which ionizing radiation (Fig. 3B) was used. When U2OS cells were released into mitosis without DNA damage, eEF2K abundance did not change (fig. S4, C and D). The change in the abundance

of eEF2K observed in response to DNA damage was not caused by an indirect cell cycle effect because eEF2K abundance remained steady during the cell cycle (fig. S4, C and D).

Treatment of U2OS cells with the proteasome inhibitor MG132 blocked the decrease of eEF2K during checkpoint silencing (Fig. 3C), indicating that the decrease in eEF2K abundance observed during checkpoint silencing was due to proteasome-dependent degradation.

To test whether βTrCP mediates eEF2K degradation during checkpoint silencing, we knocked down the expression of βTrCP in U2OS cells by RNA interference. We then synchronized U2OS cells in G_2 and induced genotoxic stress by doxorubicin treatment (Fig. 3A). βTrCP knockdown inhibited the degradation of eEF2K during checkpoint silencing (Fig. 3D). In agreement with this finding, the eEF2K-βTrCP interaction was stimulated in U2OS cells during DNA damage checkpoint silencing (Fig. 3E).

Finally, to analyze the phosphorylation of the eEF2K degron in response to genotoxic stress, we generated a phosphospecific antibody that recognizes eEF2K only when it is phosphorylated on Ser^{441} and Ser^{445} (fig. S5A). We found that phosphorylation of the eEF2K degron was induced by DNA damage in G_2 and preceded degradation of eEF2K (fig. 5SB).

Together, these findings imply that βTrCP targets eEF2K for degradation upon checkpoint silencing.

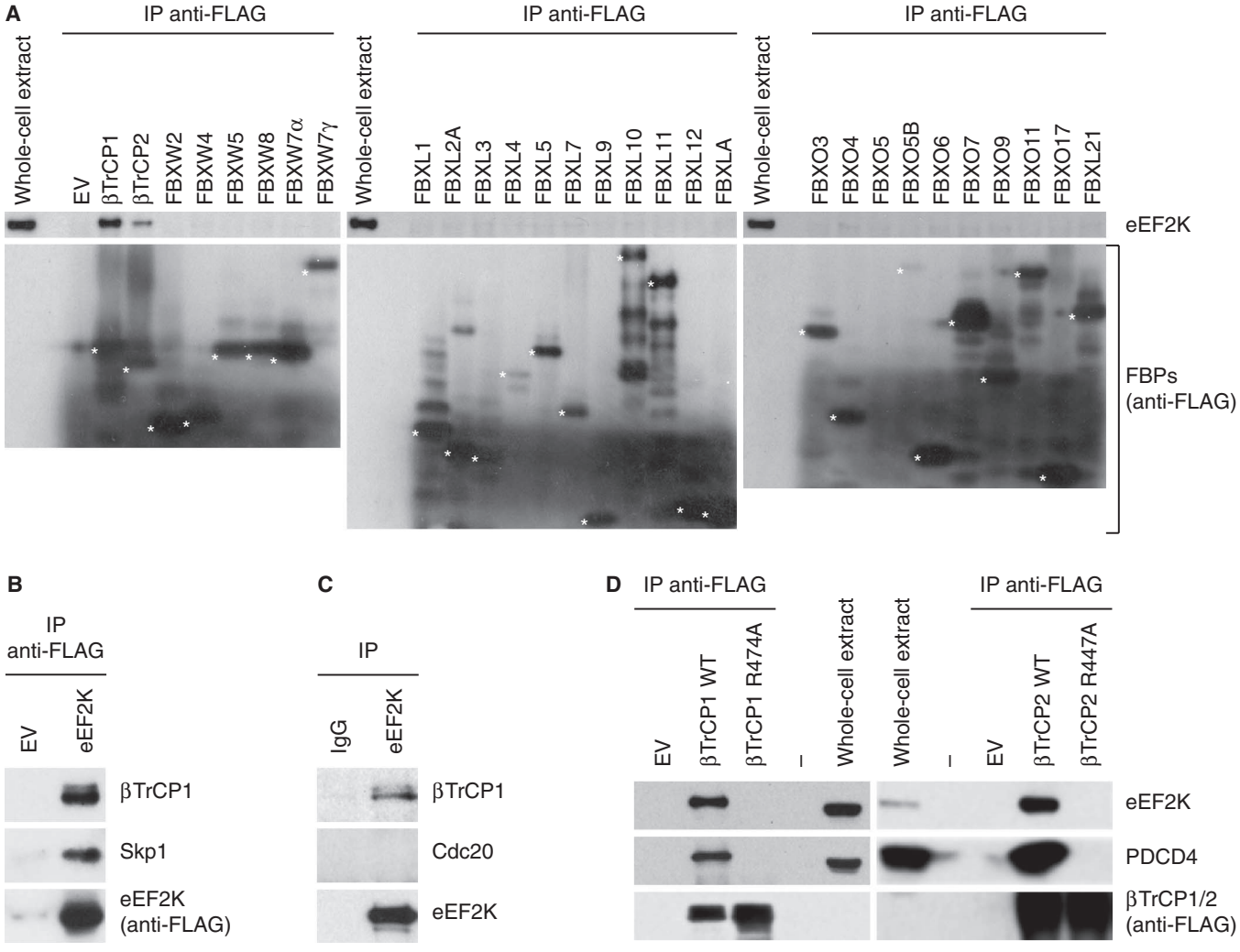

Fig. 1. eEF2K specifically associates with βTrCP1 and βTrCP2 in cells. (**A**) HEK293T cells were transfected with the indicated FLAG-tagged F-box proteins (FBPs) or an empty vector (EV) and treated with MG132 before lysis. Cell extracts were immunoprecipitated (IP) with anti-FLAG resin and immunoblotted with the indicated antibodies. (**B**) HEK293T cells were transfected with FLAG-tagged eEF2K or an empty vector and treated as in (A). (**C**) Endogenous eEF2K and βTrCP1 interact in cells. HEK293T cells were treated with MG132 before lysis. Lysates were immunoprecipitated with either an affinity-purified polyclonal antibody against eEF2K or affinity-purified immunoglobulin G (IgG) and then analyzed by immunoblotting with antibodies to the indicated proteins. (**D**) The association of βTrCP1 (left panels) and βTrCP2 (right panels) with eEF2K requires the presence of Arg^{474} in the WD40 repeat of βTrCP1 and Arg^{447} in the WD40 repeat of βTrCP2. HEK293T cells were transfected as indicated and treated as in (A). Data are representative of at least three independent experiments.

AMPK-dependent phosphorylation of eEF2K on Ser^{398} leads to activation of eEF2K in response to genotoxic stress

eEF2K controls translation elongation by phosphorylating eEF2 on Thr^{56} (*14*, *15*, *17–19*, *21–23*, *44–47*), thereby inactivating it. In addition, eEF2K-mediated phosphorylation of eEF2 on Thr^{56} inhibits the ribosome-eEF2 complex formation by reducing the affinity of eEF2 for the ribosome. Our results indicate that phosphorylation of eEF2 on Thr^{56} increases upon checkpoint activation and decreases during checkpoint silencing, mirroring the phosphorylation profile of both Chk2 on Thr^{68} (Fig. 3, A and B) and histone 2AX on Ser^{139} (Fig. 3A). To confirm that the increased phosphorylation of eEF2 on Thr^{56} in response to DNA damage is mediated by eEF2K, we silenced the expression of eEF2K in U2OS cells by RNA interference. After transfection, cells were synchronized in G_2 and then pulsed with doxorubicin for 1 hour to induce DNA damage. eEF2K knockdown blocked the DNA damage–induced phosphorylation of eEF2 on Thr^{56} (fig. S6A).

Next, we investigated the mechanism by which eEF2K-dependent phosphorylation of eEF2 is stimulated by genotoxic stress. First, to assess whether genotoxic stress stimulates the activity of eEF2K, we pulled down eEF2K from G_2 cells treated with doxorubicin and assayed immunoprecipitated eEF2K activity against in vitro translated eEF2 (Fig. 4A). The activity of eEF2K immunoprecipitated from G_2 cells treated with doxorubicin was increased when compared to eEF2K activity in G_2 cells.

eEF2K is phosphorylated on Ser^{398} by AMPK, a phosphorylation event that leads to eEF2K activation (*48*). AMPK is activated by the products of two p53 target genes, Sestrin1 and Sestrin2, in response to genotoxic stress (*49*). To test whether genotoxic stress leads to phosphorylation of eEF2K on Ser^{398}, we used a previously characterized phosphospecific antibody that can recognize eEF2K phosphorylated on Ser^{398} (*48*). U2OS

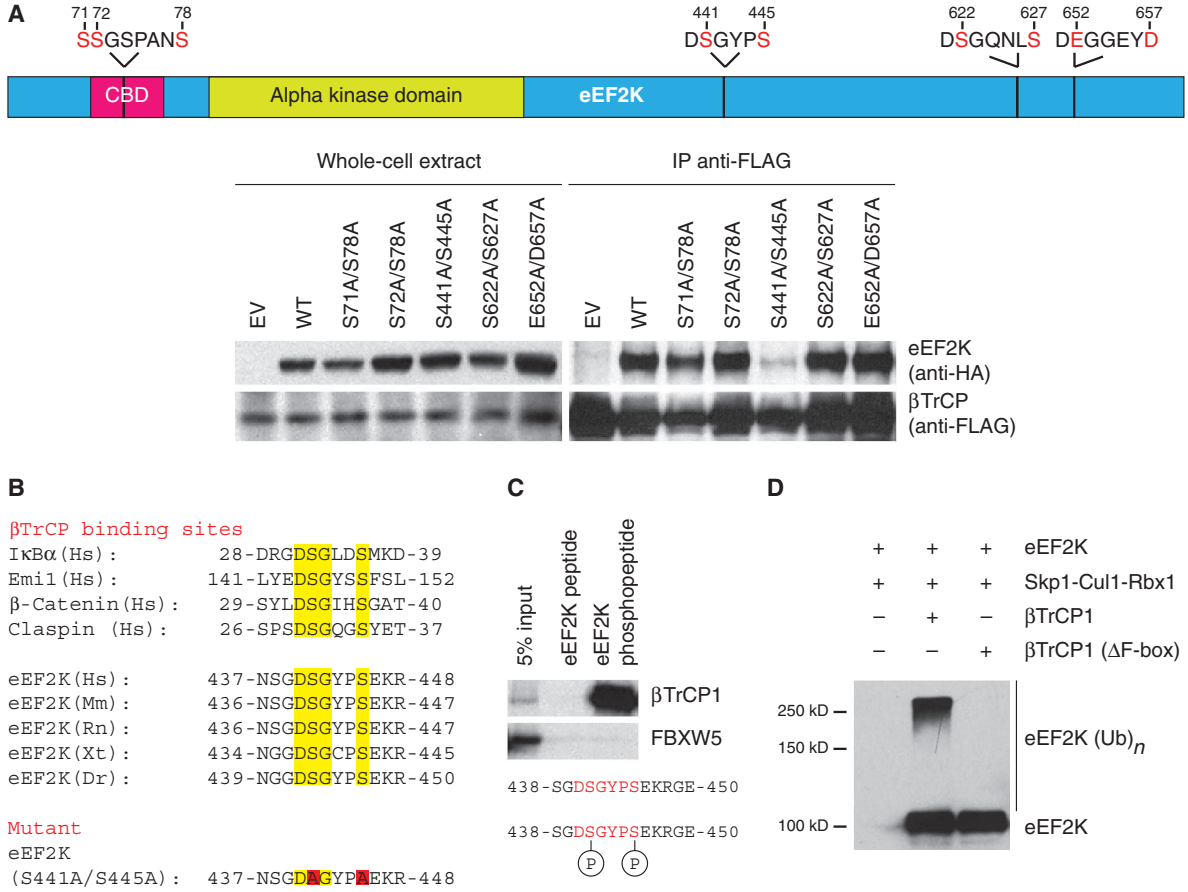

Fig. 2. The βTrCP-eEF2K interaction depends on a conserved phosphodegron. (**A**) Ser^{441} and Ser^{445} in eEF2K are required for the association with βTrCP1. Top: schematic representation of four putative eEF2K phosphodegrons. Bottom: HEK293T cells were transfected with FLAG-tagged βTrCP1 and with either an empty vector, HA-tagged eEF2K wild type (WT), or mutants, treated with MG132, and lysed. Whole-cell extracts were subjected to either immunoblotting or immunoprecipitation with anti-FLAG resin and subsequent immunoblotting. (**B**) Alignment of the amino acid regions corresponding to the βTrCP-binding motif (highlighted in yellow) in previously reported βTrCP substrates and eEF2K orthologs (top). Amino acid sequence of the eEF2K double mutant is shown (bottom). IκBα, inhibitor of nuclear factor κBα. (**C**) Phosphorylation of Ser^{441} and Ser^{445} in eEF2K is required for the interaction with βTrCP1. In vitro translated ^{35}S-labeled βTrCP1 and FBXW5 were incubated with beads coupled to the indicated eEF2K peptides. Bound proteins were eluted and subjected to electrophoresis and autoradiography. (**D**) βTrCP1 ubiquitylates eEF2K in vitro. HEK293T cells were transfected with eEF2K, Skp1, Cul1, Rbx1, and either FLAG-tagged βTrCP1 or βTrCP1(ΔF-box). In vitro ubiquitylation of eEF2K was performed with anti-FLAG immunoprecipitates, which were immunoblotted with an anti-eEF2K antibody. Data represent at least three independent experiments.

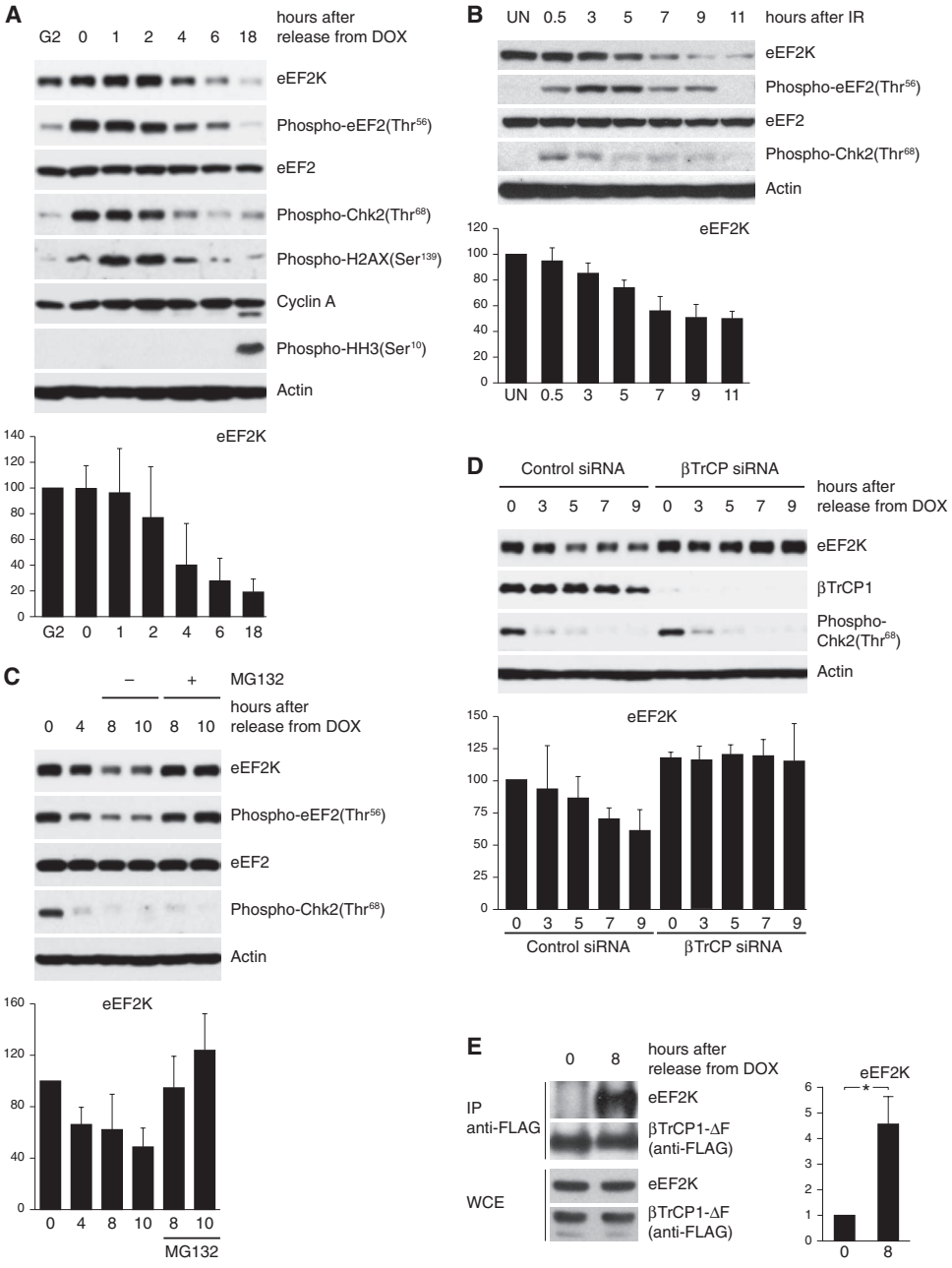

Fig. 3. βTrCP-dependent degradation of eEF2K occurs during silencing of the G_2 DNA damage checkpoint. (**A**) U2OS cells were synchronized in G_2, pulsed with doxorubicin (DOX) for 1 hour, washed, and incubated in fresh medium (indicated as time 0). Cells were harvested at the indicated time points and analyzed by immunoblotting. (**B**) U2OS cells were irradiated (10 Gy), collected at the indicated time points, and analyzed by immunoblotting (UN, untreated). (**C**) U2OS cells were treated as in (A). MG132 was added when indicated. (**D**) U2OS cells were transfected with control or βTrCP siRNAs and treated as in (A). (**E**) U2OS cells were transfected with FLAG-tagged βTrCP1(ΔF-box) or an empty vector and then treated as in (A). WCE, whole-cell extract. Graphs show eEF2K abundance normalized to a loading control and relative to the amount present at G_2 (A), in untreated (B), or at time 0 (C, D, and E). *$P < 0.01$ compared with time 0 by one-way analysis of variance (ANOVA). Data represent at least three independent experiments.

cells were synchronized in G_2 as described above and then treated with doxorubicin. Phosphorylation of eEF2K on Ser^{398} increased in response to doxorubicin treatment and was associated with increased phosphorylation of eEF2 on Thr^{56} (Fig. 4B). To examine the possibility that AMPK phosphorylates eEF2K on Ser^{398} in response to genotoxic stress, we used the AMPK inhibitor compound C (*49*, *50*). Treatment of U2OS cells with compound C blocked the increase in eEF2K phosphorylation on Ser^{398} and eEF2 phosphorylation on Thr^{56} in response to genotoxic stress (Fig. 4C). To rule out nonspecific effects of compound C, we silenced AMPKα by RNA interference and observed that AMPKα knockdown inhibited the increase in eEF2 phosphorylation on Thr^{56} in response to genotoxic stress (Fig. 4D). Together, these data indicate that genotoxic stress in G_2 cells stimulates AMPK, which phosphorylates eEF2K on Ser^{398}, causing its activation. In turn, activated eEF2K phosphorylates eEF2 on Thr^{56}, blocking its activity.

Moreover, the above results suggest that translation elongation slows down upon activation of the DNA damage checkpoint. Indeed, G_2 cells pulsed with doxorubicin exhibited increased ribosome transit time (94 s)—that is, slower rates of elongation—when compared with untreated G_2 cells (59 s; Fig. 4E).

The observed slowdown in translation elongation upon activation of the DNA damage checkpoint was associated with an eEF2K-dependent decrease in global protein synthesis as indicated by metabolic labeling of G_2 U2OS cells after genotoxic stress (fig. S6B).

Autophosphorylation of the eEF2K degron is required for its interaction with βTrCP

The above results indicate that in response to genotoxic stress, eEF2K is first activated by AMPK-mediated phosphorylation and, subsequently, during checkpoint silencing, is targeted for degradation by the ubiquitin ligase $SCF^{βTrCP}$. This sequence of events suggests a coupled activation-destruction mechanism by which eEF2K is targeted for destruction when its activity is sustained. Because eEF2K has autophosphorylation activity (*20*, *51*), we hypothesized that eEF2K, once activated, may autophosphorylate its degron, thus triggering the binding of eEF2K to βTrCP. First, to assess whether eEF2K can phosphorylate itself on Ser^{441} and Ser^{445}, eEF2K was immunopurified

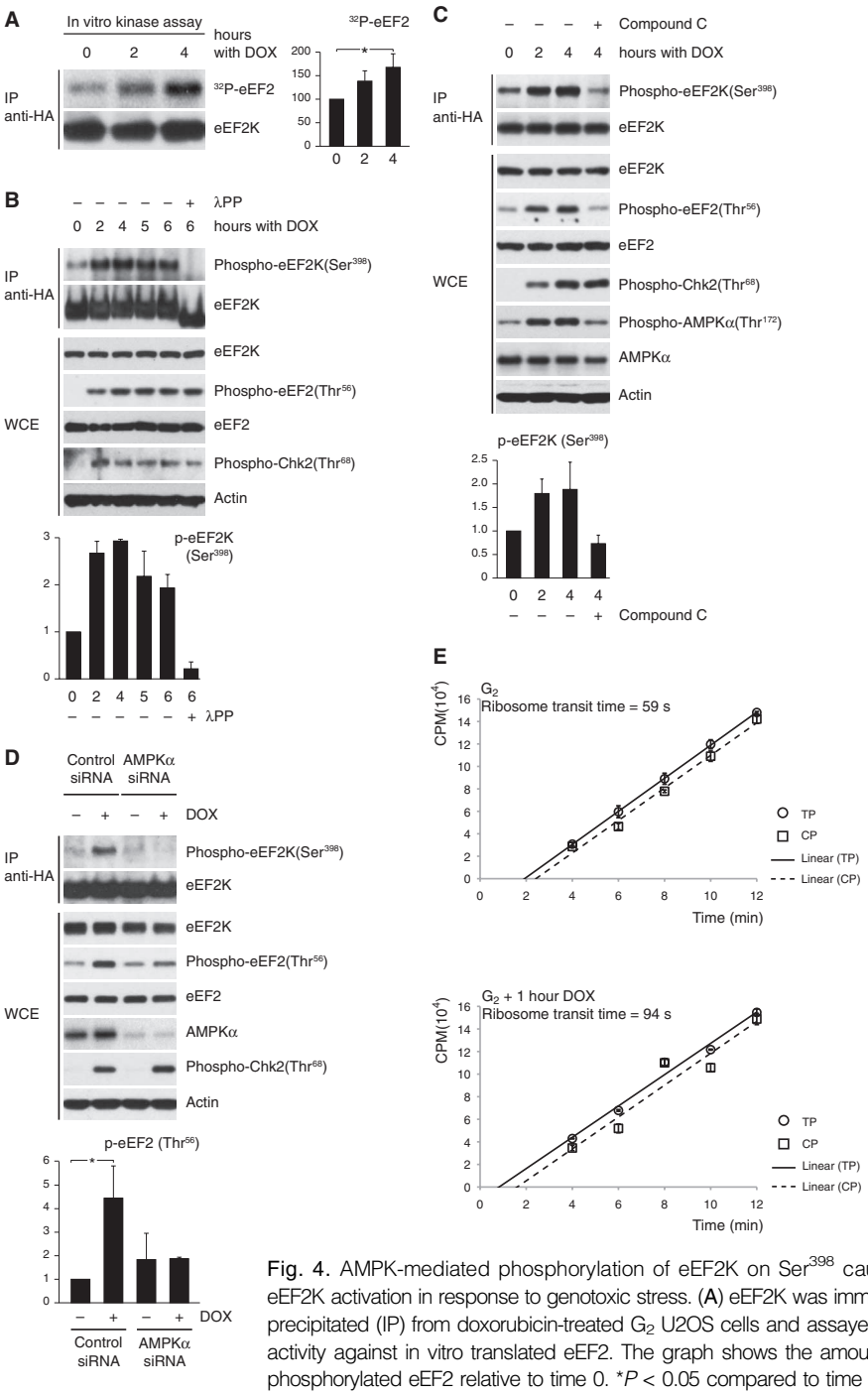

Fig. 4. AMPK-mediated phosphorylation of eEF2K on Ser[398] causes eEF2K activation in response to genotoxic stress. (**A**) eEF2K was immunoprecipitated (IP) from doxorubicin-treated G_2 U2OS cells and assayed for activity against in vitro translated eEF2. The graph shows the amount of phosphorylated eEF2 relative to time 0. *$P < 0.05$ compared to time 0 by one-way ANOVA and Dunnett's post hoc test. (**B**) G_2 U2OS cells were treated with doxorubicin for the indicated times. One IP sample (λPP) was treated with λ-phosphatase before immunoblotting. (**C** and **D**) U2OS cells were treated with compound C (C) or siRNA oligonucleotides targeting AMPKα (D). Graphs for (B) and (C) illustrate the amount of phospho-eEF2K(Ser[398]) normalized to eEF2K and relative to time 0. The graph in (D) shows the amount of phospho-eEF2(Thr[56]) normalized to eEF2 and relative to untreated control siRNA sample. *$P < 0.01$ compared to all other samples by one-way ANOVA and Bonferroni's post hoc test. (**E**) Ribosome transit time for G_2 cells and doxorubicin-treated G_2 cells. [^{35}S]Methionine incorporation into total proteins (TP; circles) or into completed peptides released from ribosomes (CP; squares) is shown (CPM, counts per minute). Comparison of ribosome transit time for G_2 and doxorubicin-treated cells by Student's *t* test gives $P < 0.005$. Data represent at least three independent experiments.

from U2OS cells, dephosphorylated, and then subjected to autophosphorylation in vitro. As a control, we used eEF2K(C314A/C318A), a kinase-dead eEF2K mutant that cannot phosphorylate either eEF2 or itself (*51*). eEF2K phosphorylation on Ser[441] and Ser[445] was then analyzed by immunoblotting with the phosphospecific antibody that recognizes eEF2K only when it is phosphorylated on Ser[441] and Ser[445]. The eEF2K degron was autophosphorylated in wild-type eEF2K but not in the kinase-dead eEF2K mutant (Fig. 5A). Similar results were obtained with eEF2K purified from *Escherichia coli* (fig. S7).

Next, we tested the ability of eEF2K (C314A/C318A) to bind βTrCP. The kinase-dead eEF2K mutant could not interact with endogenous βTrCP, analogously to the eEF2K (S441A/S445A) phosphodegron mutant (Fig. 5B). Accordingly, the eEF2K degron was phosphorylated in cells in wild-type eEF2K but not in kinase-dead eEF2K (Fig. 5B).

To exclude the possibility that the inability of eEF2K(C314A/C318A) to interact with βTrCP was indirectly caused by structural changes in eEF2K, we examined the binding of wild-type eEF2K in the presence of NH125, a specific inhibitor of eEF2K kinase activity (*52*). Treatment of U2OS with NH125 abolished both the phosphorylation of the eEF2K degron and the βTrCP binding to eEF2K (Fig. 5C) and resulted in eEF2K stabilization (Fig. 5D).

Altogether, these data strongly suggest that AMPK-mediated activation of eEF2K in response to genotoxic stress is required for eEF2K degradation during checkpoint silencing. Indeed, inhibition of AMPK by treatment with compound C prevented eEF2K degradation during checkpoint silencing (fig. S8). Although necessary, AMPK-mediated activation of eEF2K is not sufficient for eEF2K destruction because serum starvation, a well-characterized stimulus that activates AMPK, did not trigger the degradation of eEF2K (fig. S9).

Defective degradation of eEF2K delays the resumption of translation elongation during checkpoint silencing

We then asked whether βTrCP-mediated degradation of eEF2K is required to resume protein synthesis upon checkpoint silencing. U2OS cells were retrovirally transduced with HA-tagged wild-type eEF2K or HA-tagged eEF2K(S441A/S445A), synchronized in G_2 as described above, and subsequently treated with doxorubicin, released, and then collected at the indicated times. Compared to cells

expressing wild-type eEF2K and untransduced cells, cells expressing the stable eEF2K mutant that cannot bind βTrCP displayed a slower decrease in phosphorylation of eEF2 on Thr^{56} upon silencing of the DNA damage checkpoint (Fig. 6A). Similar results were obtained in cells recovering from genotoxic stress induced by ionizing irradiation (Fig. 6B). Moreover, the abundance of the kinase-dead eEF2K mutant was not decreased during checkpoint silencing (fig. S10).

Notably, during silencing of checkpoint signaling, cells expressing eEF2K(S441A/S445A) displayed a longer ribosomal transit time when compared with cells expressing wild-type eEF2K, indicating a defective resumption of the normal translation elongation rate when βTrCP-mediated degradation of eEF2K is impaired (Fig. 6C).

Next, we tested whether defective degradation of eEF2K affects global protein synthesis during checkpoint silencing. Cells expressing eEF2K(S441A/S445A) displayed a decreased rate of global protein synthesis during checkpoint silencing when compared to control cells, as measured by metabolic labeling (Fig. 6D). This difference was not observed in cells that had not been treated with doxorubicin (fig. S11), indicating that eEF2K degradation is required for efficient resumption of global protein synthesis upon silencing of the DNA damage checkpoint.

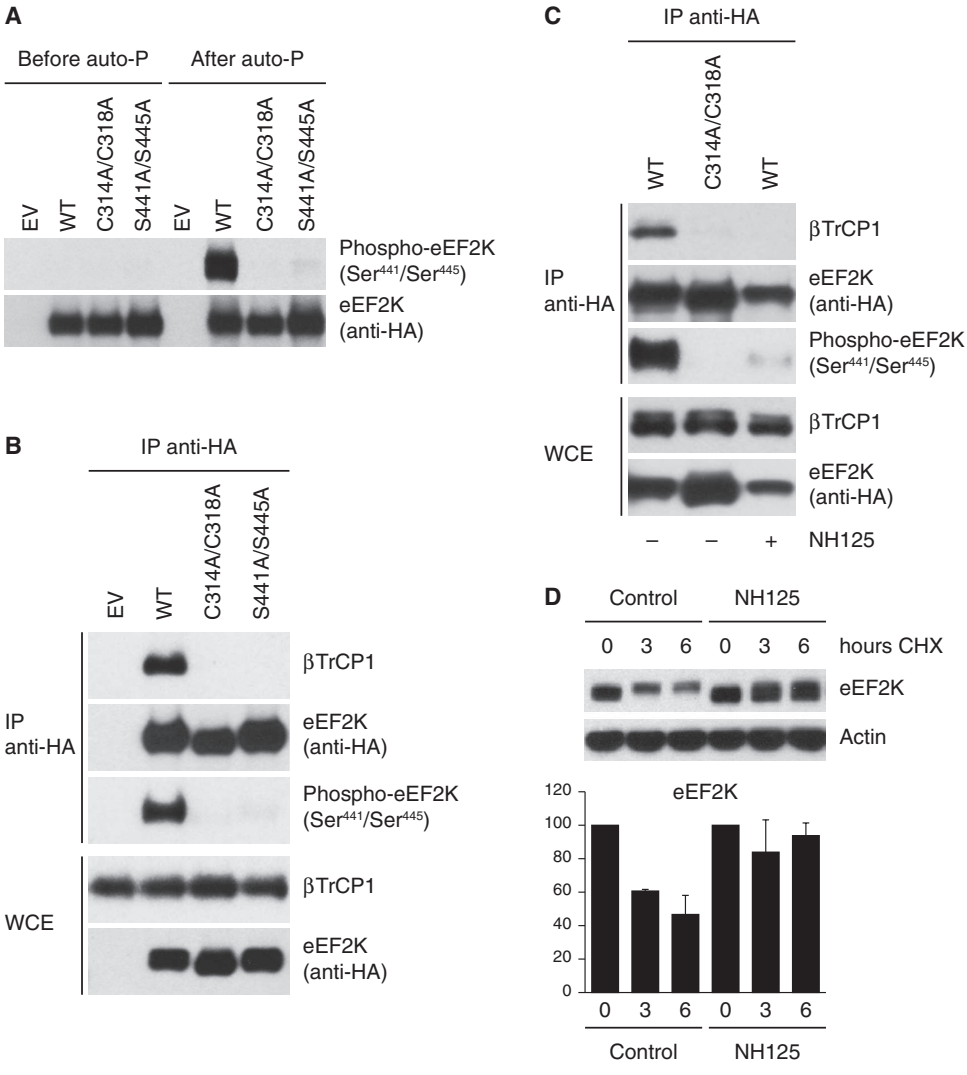

Fig. 5. eEF2K autophosphorylation on the degron triggers its binding to βTrCP. (**A**) In vitro autophosphorylation of the eEF2K degron. U2OS cells were transfected with either HA-tagged WT eEF2K, eEF2K (C314A/C318A), or eEF2K(S441A/S445A). eEF2K was purified, dephosphorylated by λ-phosphatase treatment, and then allowed to autophosphorylate in vitro. Samples were then analyzed by immunoblotting. Auto-P, autophosphorylation reaction. (**B**) Kinase-dead eEF2K mutant does not bind βTrCP1. U2OS cells were transfected with an empty vector (EV), HA-tagged WT eEF2K, eEF2K(C314A/C318A), or eEF2K (S441A/S445A). After transfection, cells were synchronized in G_2, pulsed with doxorubicin, treated with MG132, and lysed. (**C**) The βTrCP1-eEF2K interaction is blocked by an eEF2K inhibitor. U2OS cells were transfected with an empty vector or HA-tagged eEF2K. Cells were treated as in (B) and, where indicated, treated with the eEF2K inhibitor NH125. (**D**) NH125 induces the stabilization of eEF2K. Cells were pulsed with doxorubicin and treated with NH125. eEF2K turnover was analyzed by cycloheximide chase. The graph illustrates the quantification of eEF2K abundance relative to the amount at time 0. Data are representative of at least three independent experiments.

DISCUSSION

eEF2K is a ubiquitous protein kinase that plays a crucial role in the regulation of translational elongation by phosphorylating and inhibiting eEF2, a factor that promotes ribosomal translocation during the elongation phase of protein synthesis. In agreement with its key function, eEF2K activity is tightly controlled by different upstream protein kinases, which either block or stimulate its function in response to different stimuli (*24*). In addition to this level of regulation, eEF2K abundance is controlled by the ubiquitin-proteasome system (*53*); however, the biological importance of the ubiquitylation and degradation of eEF2K and the identity of the E3 ubiquitin ligase involved are unknown. Here, we show that after the activation of the DNA damage checkpoint, AMPK mediates the activation of eEF2K, which in turn phosphorylates eEF2, leading to a decrease in translation elongation rates. Subsequently, eEF2K autophosphorylation generates a phosphodegron for the recruitment of the ubiquitin ligase SCF$^{\beta TrCP}$. This event triggers the ubiquitylation of eEF2K and its proteasome-mediated degradation, which releases the inhibitory effect on eEF2 and translation elongation (Fig. 7). The coupled activation-destruction of eEF2K represents a mechanism that generates a pulse of kinase activity to dynamically tune the rate of elongation in response to genotoxic stress. This mechanism, by which eEF2K is targeted for degradation when its activity is sustained,

would imply that any condition that induces the activity of eEF2K would inevitably trigger eEF2K destruction. However, βTrCP-mediated degradation of eEF2K, which occurs specifically in response to DNA damage, suggests that additional regulatory mechanisms must exist to prevent degradation of eEF2K after other activating conditions. Possible protective roles of protein phosphatases (that counteract eEF2K autophosphorylation), deubiquitinating enzymes (that cleave ubiquitin chains conjugated on eEF2K through $SCF^{\beta TrCP}$), and chaperone proteins (that shield eEF2K from ubiquitin conjugation) in response to stress conditions different from DNA damage need to be investigated. It has been observed that eEF2K is chaperoned by Hsp90 and that cellular abundance of eEF2K is controlled by a balance between association with Hsp90 and degradation by the ubiquitin-proteasome system (*53*).

We cannot rule out that only one of the two serine residues within the eEF2K degron (Ser^{441} and Ser^{445}) is the autophosphorylation site. Indeed, liquid chromatography–MS/MS (LC-MS/MS) analysis of the eEF2K degron after in vitro autophosphorylation revealed that Ser^{445} is the predominant phosphorylated site, implying that another kinase targets Ser^{441}. According to this model, the specific degradation of eEF2K in response to DNA damage would be triggered by the cooperative actions of two kinases. The combination of eEF2K autophosphorylation (which targets Ser^{445}) and a yet to be identified kinase (that targets Ser^{441}) would be needed to generate the eEF2K phosphodegron specifically in response to DNA damage.

Regulation of translation elongation in response to DNA damage might have several advantages over controlling translation initiation. Indeed, elongation inhibition during checkpoint activation avoids the disassembly of polysomes, which, by stalling ribosomes on the mRNAs, might allow for mRNA protection from degradation or sequestration into stress granules, for example. This mechanism will also ensure that translation can rapidly resume when the checkpoint is turned off.

General inhibition of translation coupled with stimulation of translation of specific mRNA pools has been demonstrated at the levels of both initiation and elongation. For instance, DNA-PKcs (DNA-dependent protein kinase catalytic subunit)–mediated translation reprogramming in response to ultraviolet radiation allows selective synthesis of DNA damage response proteins and is based on upstream open reading frames in the 5′ untranslated region of these mRNAs (*54*). Other studies have shown that eEF2K-dependent phosphorylation of eEF2 acts to slow down the elongation step of translation and inhibits general

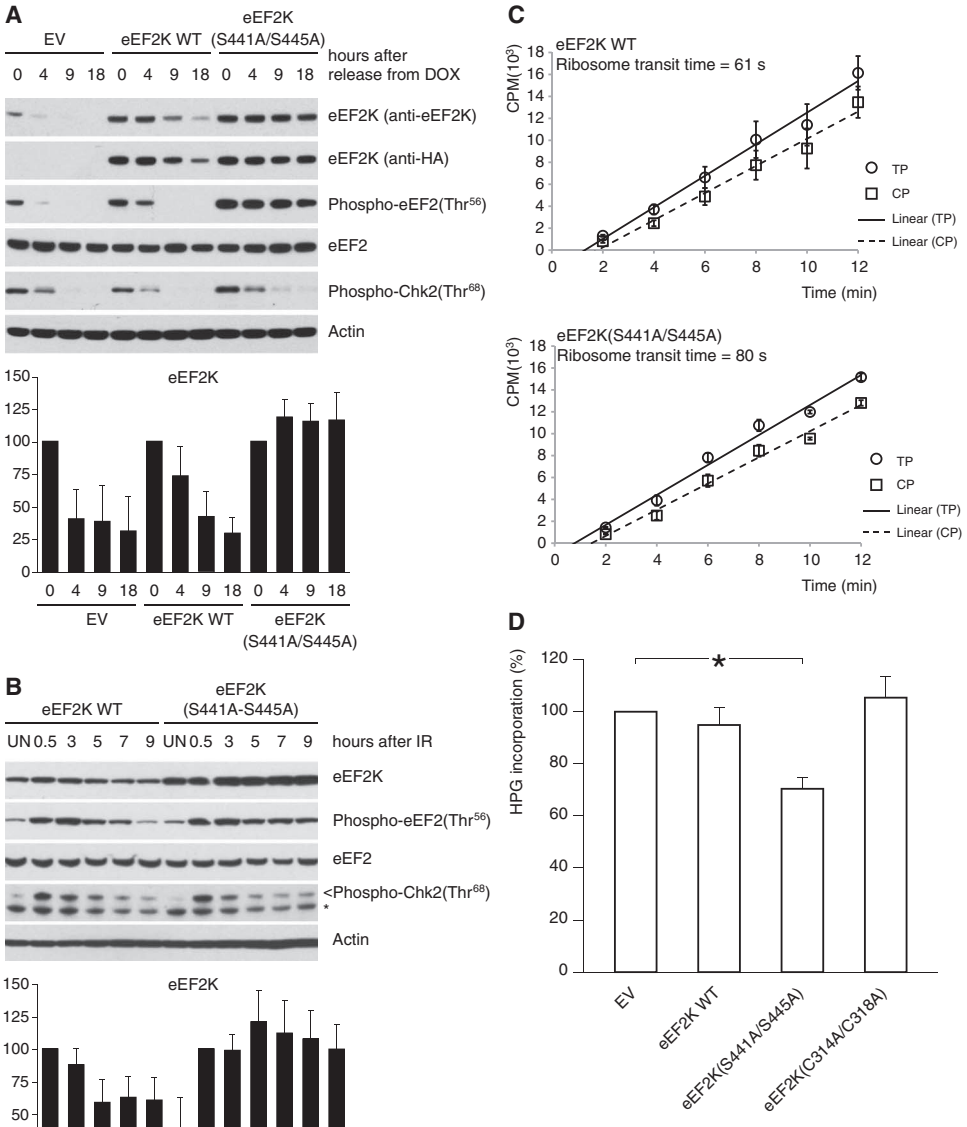

Fig. 6. Inability to degrade eEF2K delays the resumption of translation elongation during silencing of the DNA damage checkpoint. (**A**) U2OS cells were transduced with retroviruses expressing HA-tagged WT eEF2K or eEF2K(S441A/S445A), synchronized in G_2, pulsed with doxorubicin, and collected at the indicated times. Cell extracts were analyzed by immunoblotting. (**B**) U2OS cells transduced as in (A) were exposed to ionizing radiation. Cell extracts were analyzed by immunoblotting. The graphs illustrate the quantification by densitometry of eEF2K abundance relative to the amount at time 0 (A) or in untreated sample (B). (**C**) U2OS cells transduced as in (A) were collected after exposure to ionizing radiation. Incorporation of [^{35}S]methionine into total proteins (TP; circles) or into completed peptides released from ribosomes (CP; squares) is shown. Comparison of ribosome transit time for eEF2K WT and eEF2K(S441A/S445A)–expressing cells by Student's *t* test gives $P < 0.005$. (**D**) Transduced U2OS cells treated as in (A) were labeled with L-homopropargylglycine. Results are the means ± SD ($n = 3$; $^*P < 0.01$ comparing to EV by one-way ANOVA and Dunnett's post hoc test). Data represent at least three independent experiments.

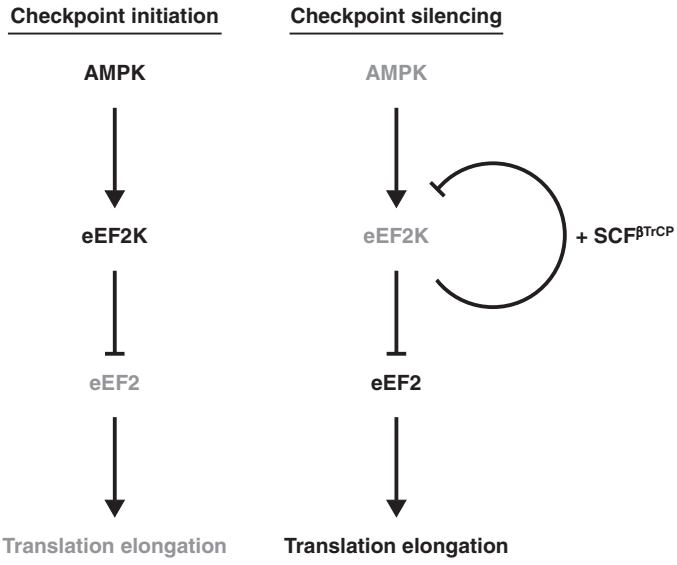

Fig. 7. Model of eEF2K regulation in response to genotoxic stress. Black lines represent activated proteins, and gray indicates inactive or degraded proteins. See text for details.

protein synthesis but simultaneously increases the translation of the mRNAs encoding Arc (activity-regulated cytoskeleton-associated protein; also known as Arg3.1), a neuronal immediate-early gene involved in both synapse plasticity and long-term potentiation (*55*). Microarray analysis of polysome- and monosome-associated mRNA pools will be required to identify mRNAs that are translated only during the DNA damage checkpoint.

$SCF^{\beta TrCP}$ is implicated in the degradation of several substrates during the recovery from DNA damage and replication stress checkpoints. Indeed, βTrCP is required to reactivate the cyclin-dependent kinase Cdk1 by targeting the Cdk1 inhibitors Claspin and Wee1 for proteasome-dependent degradation (*35*, *41*, *56–60*) and turn off the DNA repair machinery by causing the destruction of the Fanconi anemia protein FANCM (*61*). Our findings show that βTrCP is also needed during checkpoint silencing to resume protein synthesis by triggering proteolysis of eEF2K, suggesting that the ubiquitin ligase $SCF^{\beta TrCP}$ coordinates different processes (such as cell cycle progression, DNA repair, and protein synthesis) that are critical for checkpoint termination.

MATERIALS AND METHODS

Cell culture, synchronization, and drug treatment

HEK293T, 293GP2, and U2OS cells were maintained in Dulbecco's modified Eagle's medium (DMEM; Invitrogen) containing 10% fetal calf serum. HCT116, SW480, and MCF7 cells were maintained in DMEM/Nutrient Mixture F-12 (DMEM/F-12) containing 10% fetal calf serum. Synchronizations and flow analysis were performed as described (*38*). MG132 (10 μM) was added when indicated.

Biochemical methods

Extract preparation, immunoprecipitation, and immunoblotting were performed as previously described (*33*, *40*).

Purification of βTrCP2 interactors

HEK293T cells were transfected with pcDNA3-FLAG-HA-βTrCP2 and treated with 10 μM MG132 for 5 hours. Cells were harvested and subsequently lysed in lysis buffer [50 mM tris-HCl (pH 7.5), 150 mM NaCl, 1 mM EDTA, and 0.5% NP-40 plus protease and phosphatase inhibitors]. βTrCP2 was immunopurified with anti-FLAG agarose resin (Sigma). Beads were washed, and proteins were eluted by competition with FLAG peptide (Sigma). The eluate was then subjected to a second immunopurification with anti-HA resin (12CA5 monoclonal antibody cross-linked to protein G–Sepharose; Invitrogen) before elution in Laemmli sample buffer. The final eluate was separated by SDS–polyacrylamide gel electrophoresis (SDS-PAGE), and proteins were visualized by Coomassie colloidal blue. Bands were sliced out from the gels and subjected to in-gel digestion. Gel pieces were then reduced, alkylated, and digested according to a published protocol (*62*). For mass spectrometric analysis, peptides recovered from in-gel digestion were separated with a C18 column and introduced by nano-electrospray into an LTQ Orbitrap XL mass spectrometer (Thermo Fisher). Peak lists were generated from the MS/MS spectra with MaxQuant (*63*), and then searched against the International Protein Index human database with Mascot search engine (Matrix Science). Carbaminomethylation (+57 daltons) was set as fixed modification and protein N-terminal acetylation and methionine oxidation as variable modifications. Peptide tolerance was set to 7 parts per million (ppm) and fragment ion tolerance was set to 0.5 daltons, allowing two missed cleavages with trypsin enzyme.

Antibodies

Mouse monoclonal antibodies were from Invitrogen (Cul1), Sigma (FLAG, eEF2K), Santa Cruz Biotechnology (actin), BD (β-catenin, p27), and Covance (HA). Rabbit polyclonal antibodies were from Bethyl (PDCD4), Cell Signaling [βTrCP1, eEF2K, eEF2, phospho-eEF2(Thr^{56}), phospho-Chk2(Thr^{68})], Millipore [phospho-histone H3(Ser^{10}), phospho-histone H2AX(Ser^{139})], Sigma (FLAG, USP8), Novus Biologicals (HIF1α), and Santa Cruz (cyclin A, Cdc20, Skp1, and HA).

Plasmids

eEF2K mutants were generated with the QuikChange Site-Directed Mutagenesis kit (Stratagene). For retrovirus production, both wild-type eEF2K and eEF2K mutants were subcloned into the retroviral vector pBABEpuro. All complementary DNAs (cDNAs) were sequenced.

Transient transfections and retrovirus-mediated gene transfer

HEK293T cells were transfected with the calcium phosphate method as described (*33*, *40*). Retrovirus-mediated gene transfer was performed as previously described (*33*, *40*).

Gene silencing by small interfering RNA

The sequence and validation of the oligonucleotides corresponding to βTrCP1 and βTrCP2 were previously published (*33*, *40*, *41*, *64*). Both eEF2K and AMPKα SMARTpool small interfering RNA (siRNA) oligonucleotides were from Dharmacon. Cells were transfected with the oligos twice (24 and 48 hours after plating) by the use of Oligofectamine (Invitrogen) according to the manufacturer's recommendations. Forty-eight hours after the last transfection, lysates were prepared and analyzed by SDS-PAGE and immunoblotting.

In vitro ubiquitylation assay

eEF2K ubiquitylation was performed in a volume of 10 μl containing $SCF^{\beta TrCP}$-eEF2K immunocomplexes, 50 mM tris (pH 7.6), 5 mM $MgCl_2$, 0.6 mM dithiothreitol (DTT), 2 mM adenosine triphosphate (ATP), 2 μl of in vitro translated unlabeled βTrCP1, E1 (1.5 ng/μl; Boston Biochem), Ubc3 (10 ng/μl), ubiquitin (2.5 μg/μl; Sigma), and 1 μM

ubiquitin aldehyde. The reactions were incubated at 30°C for the indicated times and analyzed by immunoblotting. In the assay shown in fig. S3, ^{35}S-labeled in vitro translated eEF2K [wild type or eEF2K(S441A/S445A)] was used instead of immunoprecipitated eEF2K. The reactions were analyzed by SDS-PAGE and autoradiography.

Phosphorylation analysis of the eEF2K degron in cells

FLAG-eEF2K was coexpressed with the Cul1 dominant-negative deletion mutant CUL1-N252, and immunopurified. FLAG immunocomplexes were eluted with 8 M urea. Samples were then reduced with 10 mM DTT for 30 min at 60°C followed by addition of iodoacetamide to 20 mM followed by 30-min incubation in the dark at room temperature. The first digestion was performed with Lys-C for 4 hours at 37°C. Subsequently, the digest was diluted fivefold with 50 mM ammonium bicarbonate to a final urea concentration of less than 2 M, and a second digestion with trypsin was performed overnight at 37°C. Finally, the digestion was quenched by addition of formic acid to a final concentration of 0.1% (vol/vol). The resulting solution was desalted with 200-mg Sep-Pak C18 cartridges (Waters Corporation), lyophilized, and stored at −20°C.

Ti-IMAC microcolumns were prepared as previously described (*65*). Trypsinized peptides were loaded onto preconditioned microcolumns, which were later sequentially washed with 60 μl of loading buffer followed by 60 μl of 50% acetonitrile (ACN)/0.5% trifluoroacetic acid (TFA) containing 200 mM NaCl and 60 μl of 50% ACN/0.1% TFA. The bound peptides were eluted by 20 μl of 5% ammonia into 20 μl of 10% formic acid and then stored at −20°C before LC-MS/MS analysis. MS spectra assignment was performed with MaxQuant version 1.1.1.25.

In vitro kinase assay

eEF2K kinase activity was assayed as described (*48*).

Ribosome transit time measurements

The method for ribosome transit time measurements is adapted from (*45*, *66*). In brief, cells were incubated in methionine-free medium for 30 min before addition of labeling medium containing L-[^{35}S]methionine (10 μCi/ml) (NEG709A, PerkinElmer). Samples were harvested in phosphate-buffered saline (PBS) containing cycloheximide (100 μg/ml) at 2, 4, 6, 8, 10, and 12 min after labeling and pelleted. Cell lysis and pelleting of polysomes were executed as described (*66*). Polysomes were pelleted at 55,000*g* for 20 min at 4°C in a Beckman Sw55Ti rotor.

Fifty microliters of the total protein fraction (postmitochondrial supernatant) and completed protein fraction (postribosomal supernatant) was loaded on 3MM paper and precipitated by consecutive incubations in cold 10% trichloroacetic acid (TCA) and boiling 10% TCA (2.5 min per step) and briefly washed in acetone and ethanol. Filters were air-dried, and incorporation of [^{35}S]methionine was measured by liquid scintillation counting (three measurements per sample).

To calculate ribosome transit times, we measured the lag between the linear incorporation of labeled methionine in total protein (TP) and the linear incorporation in complete protein (CP), which represents the time it takes for all nascent peptides to be labeled (*67*). This lag is seen in the graph as the difference in x intercepts of the two extrapolated lines and represents the half-transit time (half because the average length of polypeptides on a polyribosome is always half of the full length of completed peptides). To obtain the ribosome transit time, we doubled the difference in intercepts.

Metabolic labeling

U2OS cells were cultured in methionine-free medium for 60 min and then incubated in 50 μM Click-iT HPG (L-homopropargylglycine) for 90 min. Cells were fixed in 70% ethanol, stained with Alexa Fluor 488 azide, and analyzed by fluorescence-activated cell sorting.

Statistical analysis

All data shown are from one representative experiment of at least three performed. Statistical tests used are specified in the legends of relevant figures.

SUPPLEMENTARY MATERIALS

www.sciencesignaling.org/cgi/content/full/5/227/ra40/DC1

Fig. S1. eEF2K interacts with βTrCP1 and βTrCP2.
Fig. S2. Phosphorylation of the eEF2K degron in cells.
Fig. S3. βTrCP-mediated ubiquitylation of eEF2K depends on an intact phosphodegron.
Fig. S4. eEF2K abundance in response to mitogens and during the cell cycle.
Fig. S5. The eEF2K degron is phosphorylated in response to genotoxic stress.
Fig. S6. DNA damage–dependent phosphorylation of eEF2 on Thr^{56} and decreased protein synthesis are mediated by eEF2K.
Fig. S7. In vitro autophosphorylation of the eEF2K degron.
Fig. S8. AMPK inhibition prevents eEF2K degradation during checkpoint silencing.
Fig. S9. Serum starvation, a stimulus that activates AMPK, does not lead to eEF2K degradation.
Fig. S10. The kinase-dead eEF2K mutant is not degraded during checkpoint silencing.
Fig. S11. Expression of the eEF2K(S441A/S445A) mutant in exponentially growing U2OS cells does not lead to decreased protein synthesis.

REFERENCES AND NOTES

1. J. Bartek, J. Lukas, DNA damage checkpoints: From initiation to recovery or adaptation. *Curr. Opin. Cell Biol.* **19**, 238–245 (2007).
2. J. W. Harper, S. J. Elledge, The DNA damage response: Ten years after. *Mol. Cell* **28**, 739–745 (2007).
3. X. Lü, L. de la Peña, C. Barker, K. Camphausen, P. J. Tofilon, Radiation-induced changes in gene expression involve recruitment of existing messenger RNAs to and away from polysomes. *Cancer Res.* **66**, 1052–1061 (2006).
4. F. Buttgereit, M. D. Brand, A hierarchy of ATP-consuming processes in mammalian cells. *Biochem. J.* **312** (Pt. 1), 163–167 (1995).
5. A. Efeyan, D. M. Sabatini, mTOR and cancer: Many loops in one pathway. *Curr. Opin. Cell Biol.* **22**, 169–176 (2010).
6. D. D. Sarbassov, S. M. Ali, D. M. Sabatini, Growing roles for the mTOR pathway. *Curr. Opin. Cell Biol.* **17**, 596–603 (2005).
7. G. J. Browne, C. G. Proud, Regulation of peptide-chain elongation in mammalian cells. *Eur. J. Biochem.* **269**, 5360–5368 (2002).
8. G. J. Browne, C. G. Proud, A novel mTOR-regulated phosphorylation site in elongation factor 2 kinase modulates the activity of the kinase and its binding to calmodulin. *Mol. Cell. Biol.* **24**, 2986–2997 (2004).
9. E. Connolly, S. Braunstein, S. Formenti, R. J. Schneider, Hypoxia inhibits protein synthesis through a 4E-BP1 and elongation factor 2 kinase pathway controlled by mTOR and uncoupled in breast cancer cells. *Mol. Cell. Biol.* **26**, 3955–3965 (2006).
10. W. N. Hait, H. Wu, S. Jin, J. M. Yang, Elongation factor-2 kinase: Its role in protein synthesis and autophagy. *Autophagy* **2**, 294–296 (2006).
11. C. G. Proud, Regulation of mammalian translation factors by nutrients. *Eur. J. Biochem.* **269**, 5338–5349 (2002).
12. C. G. Proud, Control of the translational machinery in mammalian cells. *Eur. J. Biochem.* **269**, 5337 (2002).
13. N. T. Redpath, N. T. Price, C. G. Proud, Cloning and expression of cDNA encoding protein synthesis elongation factor-2 kinase. *J. Biol. Chem.* **271**, 17547–17554 (1996).
14. U. Carlberg, A. Nilsson, O. Nygård, Functional properties of phosphorylated elongation factor 2. *Eur. J. Biochem.* **191**, 639–645 (1990).
15. K. Mitsui, M. Brady, H. C. Palfrey, A. C. Nairn, Purification and characterization of calmodulin-dependent protein kinase III from rabbit reticulocytes and rat pancreas. *J. Biol. Chem.* **268**, 13422–13433 (1993).
16. A. C. Nairn, B. Bhagat, H. C. Palfrey, Identification of calmodulin-dependent protein kinase III and its major M_r 100,000 substrate in mammalian tissues. *Proc. Natl. Acad. Sci. U.S.A.* **82**, 7939–7943 (1985).
17. A. C. Nairn, M. Matsushita, K. Nastiuk, A. Horiuchi, K. Mitsui, Y. Shimizu, H. C. Palfrey, Elongation factor-2 phosphorylation and the regulation of protein synthesis by calcium. *Prog. Mol. Subcell. Biol.* **27**, 91–129 (2001).

18. L. P. Ovchinnikov, L. P. Motuz, P. G. Natapov, L. J. Averbuch, R. E. Wettenhall, R. Szyszka, G. Kramer, B. Hardesty, Three phosphorylation sites in elongation factor 2. *FEBS Lett.* **275**, 209–212 (1990).
19. N. T. Price, N. T. Redpath, K. V. Severinov, D. G. Campbell, J. M. Russell, C. G. Proud, Identification of the phosphorylation sites in elongation factor-2 from rabbit reticulocytes. *FEBS Lett.* **282**, 253–258 (1991).
20. N. T. Redpath, C. G. Proud, Purification and phosphorylation of elongation factor-2 kinase from rabbit reticulocytes. *Eur. J. Biochem.* **212**, 511–520 (1993).
21. A. G. Ryazanov, P. G. Natapov, E. A. Shestakova, F. F. Severin, A. S. Spirin, Phosphorylation of the elongation factor 2: The fifth Ca^{2+}/calmodulin-dependent system of protein phosphorylation. *Biochimie* **70**, 619–626 (1988).
22. A. G. Ryazanov, E. A. Shestakova, P. G. Natapov, Phosphorylation of elongation factor 2 by EF-2 kinase affects rate of translation. *Nature* **334**, 170–173 (1988).
23. A. G. Ryazanov, M. D. Ward, C. E. Mendola, K. S. Pavur, M. V. Dorovkov, M. Wiedmann, H. Erdjument-Bromage, P. Tempst, T. G. Parmer, C. R. Prostko, F. J. Germino, W. N. Hait, Identification of a new class of protein kinases represented by eukaryotic elongation factor-2 kinase. *Proc. Natl. Acad. Sci. U.S.A.* **94**, 4884–4889 (1997).
24. X. Wang, C. G. Proud, The mTOR pathway in the control of protein synthesis. *Physiology* **21**, 362–369 (2006).
25. L. E. Horton, M. Bushell, D. Barth-Baus, V. J. Tilleray, M. J. Clemens, J. O. Hensold, p53 activation results in rapid dephosphorylation of the eIF4E-binding protein 4E-BP1, inhibition of ribosomal protein S6 kinase and inhibition of translation initiation. *Oncogene* **21**, 5325–5334 (2002).
26. Z. Feng, H. Zhang, A. J. Levine, S. Jin, The coordinate regulation of the p53 and mTOR pathways in cells. *Proc. Natl. Acad. Sci. U.S.A.* **102**, 8204–8209 (2005).
27. M. B. Kastan, J. Bartek, Cell-cycle checkpoints and cancer. *Nature* **432**, 316–323 (2004).
28. A. Hershko, A. Ciechanover, The ubiquitin system. *Annu. Rev. Biochem.* **67**, 425–479 (1998).
29. M. D. Petroski, R. J. Deshaies, Function and regulation of cullin-RING ubiquitin ligases. *Nat. Rev. Mol. Cell Biol.* **6**, 9–20 (2005).
30. D. Frescas, M. Pagano, Deregulated proteolysis by the F-box proteins SKP2 and β-TrCP: Tipping the scales of cancer. *Nat. Rev. Cancer* **8**, 438–449 (2008).
31. T. Cardozo, M. Pagano, The SCF ubiquitin ligase: Insights into a molecular machine. *Nat. Rev. Mol. Cell Biol.* **5**, 739–751 (2004).
32. G. Wu, G. Xu, B. A. Schulman, P. D. Jeffrey, J. W. Harper, N. P. Pavletich, Structure of a β-TrCP1-Skp1-β-catenin complex: Destruction motif binding and lysine specificity of the $SCF^{β\text{-}TrCP1}$ ubiquitin ligase. *Mol. Cell* **11**, 1445–1456 (2003).
33. D. Guardavaccaro, D. Frescas, N. V. Dorrello, A. Peschiaroli, A. S. Multani, T. Cardozo, A. Lasorella, A. Iavarone, S. Chang, E. Hernando, M. Pagano, Control of chromosome stability by the β-TrCP–REST–Mad2 axis. *Nature* **452**, 365–369 (2008).
34. Y. Kanemori, K. Uto, N. Sagata, β-TrCP recognizes a previously undescribed nonphosphorylated destruction motif in Cdc25A and Cdc25B phosphatases. *Proc. Natl. Acad. Sci. U.S.A.* **102**, 6279–6284 (2005).
35. N. Watanabe, H. Arai, Y. Nishihara, M. Taniguchi, N. Watanabe, T. Hunter, H. Osada, M-phase kinases induce phospho-dependent ubiquitination of somatic Wee1 by SCFβ-TrCP. *Proc. Natl. Acad. Sci. U.S.A.* **101**, 4419–4424 (2004).
36. P. J. Boersema, S. Mohammed, A. J. Heck, Phosphopeptide fragmentation and analysis by mass spectrometry. *J. Mass Spectrom.* **44**, 861–878 (2009).
37. R. Piva, J. Liu, R. Chiarle, A. Podda, M. Pagano, G. Inghirami, In vivo interference with Skp1 function leads to genetic instability and neoplastic transformation. *Mol. Cell. Biol.* **22**, 8375–8387 (2002).
38. D. Guardavaccaro, Y. Kudo, J. Boulaire, M. Barchi, L. Busino, M. Donzelli, F. Margottin-Goguet, P. K. Jackson, L. Yamasaki, M. Pagano, Control of meiotic and mitotic progression by the F box protein β-Trcp1 in vivo. *Dev. Cell* **4**, 799–812 (2003).
39. L. Busino, M. Donzelli, M. Chiesa, D. Guardavaccaro, D. Ganoth, N. V. Dorrello, A. Hershko, M. Pagano, G. F. Draetta, Degradation of Cdc25A by β-TrCP during S phase and in response to DNA damage. *Nature* **426**, 87–91 (2003).
40. N. V. Dorrello, A. Peschiaroli, D. Guardavaccaro, N. H. Colburn, N. E. Sherman, M. Pagano, S6K1- and βTRCP-mediated degradation of PDCD4 promotes protein translation and cell growth. *Science* **314**, 467–471 (2006).
41. A. Peschiaroli, N. V. Dorrello, D. Guardavaccaro, M. Venere, T. Halazonetis, N. E. Sherman, M. Pagano, $SCF^{βTrCP}$-mediated degradation of Claspin regulates recovery from the DNA replication checkpoint response. *Mol. Cell* **23**, 319–329 (2006).
42. G. Sivan, N. Kedersha, O. Elroy-Stein, Ribosomal slowdown mediates translational arrest during cellular division. *Mol. Cell. Biol.* **27**, 6639–6646 (2007).
43. X. Wang, W. Li, M. Williams, N. Terada, D. R. Alessi, C. G. Proud, Regulation of elongation factor 2 kinase by $p90^{RSK1}$ and p70 S6 kinase. *EMBO J.* **20**, 4370–4379 (2001).
44. D. M. Bagaglio, E. H. Cheng, F. S. Gorelick, K. Mitsui, A. C. Nairn, W. N. Hait, Phosphorylation of elongation factor 2 in normal and malignant rat glial cells. *Cancer Res.* **53**, 2260–2264 (1993).
45. N. T. Redpath, E. J. Foulstone, C. G. Proud, Regulation of translation elongation factor-2 by insulin via a rapamycin-sensitive signalling pathway. *EMBO J.* **15**, 2291–2297 (1996).
46. N. T. Redpath, N. T. Price, K. V. Severinov, C. G. Proud, Regulation of elongation factor-2 by multisite phosphorylation. *Eur. J. Biochem.* **213**, 689–699 (1993).
47. A. G. Ryazanov, E. K. Davydova, Mechanism of elongation factor 2 (EF-2) inactivation upon phosphorylation. Phosphorylated EF-2 is unable to catalyze translocation. *FEBS Lett.* **251**, 187–190 (1989).
48. G. J. Browne, S. G. Finn, C. G. Proud, Stimulation of the AMP-activated protein kinase leads to activation of eukaryotic elongation factor 2 kinase and to its phosphorylation at a novel site, serine 398. *J. Biol. Chem.* **279**, 12220–12231 (2004).
49. A. V. Budanov, M. Karin, p53 target genes sestrin1 and sestrin2 connect genotoxic stress and mTOR signaling. *Cell* **134**, 451–460 (2008).
50. G. Zhou, R. Myers, Y. Li, Y. Chen, X. Shen, J. Fenyk-Melody, M. Wu, J. Ventre, T. Doebber, N. Fujii, N. Musi, M. F. Hirshman, L. J. Goodyear, D. E. Moller, Role of AMP-activated protein kinase in mechanism of metformin action. *J. Clin. Invest.* **108**, 1167–1174 (2001).
51. T. A. Diggle, C. K. Seehra, S. Hase, N. T. Redpath, Analysis of the domain structure of elongation factor-2 kinase by mutagenesis. *FEBS Lett.* **457**, 189–192 (1999).
52. S. Arora, J. M. Yang, T. G. Kinzy, R. Utsumi, T. Okamoto, T. Kitayama, P. A. Ortiz, W. N. Hait, Identification and characterization of an inhibitor of eukaryotic elongation factor 2 kinase against human cancer cell lines. *Cancer Res.* **63**, 6894–6899 (2003).
53. S. Arora, J. M. Yang, W. N. Hait, Identification of the ubiquitin-proteasome pathway in the regulation of the stability of eukaryotic elongation factor-2 kinase. *Cancer Res.* **65**, 3806–3810 (2005).
54. I. R. Powley, A. Kondrashov, L. A. Young, H. C. Dobbyn, K. Hill, I. G. Cannell, M. Stoneley, Y. W. Kong, J. A. Cotes, G. C. Smith, R. Wek, C. Hayes, T. W. Gant, K. A. Spriggs, M. Bushell, A. E. Willis, Translational reprogramming following UVB irradiation is mediated by DNA-PKcs and allows selective recruitment to the polysomes of mRNAs encoding DNA repair enzymes. *Genes Dev.* **23**, 1207–1220 (2009).
55. S. Park, J. M. Park, S. Kim, J. A. Kim, J. D. Shepherd, C. L. Smith-Hicks, S. Chowdhury, W. Kaufmann, D. Kuhl, A. G. Ryazanov, R. L. Huganir, D. J. Linden, P. F. Worley, Elongation factor 2 and fragile X mental retardation protein control the dynamic translation of Arc/Arg3.1 essential for mGluR-LTD. *Neuron* **59**, 70–83 (2008).
56. R. Freire, M. A. van Vugt, I. Mamely, R. H. Medema, Claspin: Timing the cell cycle arrest when the genome is damaged. *Cell Cycle* **5**, 2831–2834 (2006).
57. N. Mailand, S. Bekker-Jensen, J. Bartek, J. Lukas, Destruction of Claspin by $SCF^{βTrCP}$ restrains Chk1 activation and facilitates recovery from genotoxic stress. *Mol. Cell* **23**, 307–318 (2006).
58. I. Mamely, M. A. van Vugt, V. A. Smits, J. I. Semple, B. Lemmens, A. Perrakis, R. H. Medema, R. Freire, Polo-like kinase-1 controls proteasome-dependent degradation of Claspin during checkpoint recovery. *Curr. Biol.* **16**, 1950–1955 (2006).
59. J. Jin, T. Shirogane, L. Xu, G. Nalepa, J. Qin, S. J. Elledge, J. W. Harper, $SCF^{β\text{-}TRCP}$ links Chk1 signaling to degradation of the Cdc25A protein phosphatase. *Genes Dev.* **17**, 3062–3074 (2003).
60. N. Watanabe, H. Arai, J. Iwasaki, M. Shiina, K. Ogata, T. Hunter, H. Osada, Cyclin-dependent kinase (CDK) phosphorylation destabilizes somatic Wee1 via multiple pathways. *Proc. Natl. Acad. Sci. U.S.A.* **102**, 11663–11668 (2005).
61. Y. Kee, J. M. Kim, A. D. D'Andrea, Regulated degradation of FANCM in the Fanconi anemia pathway during mitosis. *Genes Dev.* **23**, 555–560 (2009).
62. A. Shevchenko, M. Wilm, O. Vorm, M. Mann, Mass spectrometric sequencing of proteins silver-stained polyacrylamide gels. *Anal. Chem.* **68**, 850–858 (1996).
63. J. Cox, M. Mann, MaxQuant enables high peptide identification rates, individualized p.p.b.-range mass accuracies and proteome-wide protein quantification. *Nat. Biotechnol.* **26**, 1367–1372 (2008).
64. F. Bassermann, D. Frescas, D. Guardavaccaro, L. Busino, A. Peschiaroli, M. Pagano, The Cdc14B-Cdh1-Plk1 axis controls the G2 DNA-damage-response checkpoint. *Cell* **134**, 256–267 (2008).
65. H. Zhou, M. Ye, J. Dong, G. Han, X. Jiang, R. Wu, H. Zou, Specific phosphopeptide enrichment with immobilized titanium ion affinity chromatography adsorbent for phosphoproteome analysis. *J. Proteome Res.* **7**, 3957–3967 (2008).
66. I. Ruvinsky, N. Sharon, T. Lerer, H. Cohen, M. Stolovich-Rain, T. Nir, Y. Dor, P. Zisman, O. Meyuhas, Ribosomal protein S6 phosphorylation is a determinant of cell size and glucose homeostasis. *Genes Dev.* **19**, 2199–2211 (2005).
67. P. J. Nielsen, E. H. McConkey, Evidence for control of protein synthesis in HeLa cells via the elongation rate. *J. Cell. Physiol.* **104**, 269–281 (1980).

Acknowledgments: We thank W. N. Hait, M. Innocenti, N. V. Dorrello, R. H. Giles, and H. Zhou for their contributions and R. H. Medema and D. Frescas for critically reading the manuscript. **Funding:** Work in D.G.'s laboratory is supported by the Royal Dutch Academy of Arts and Sciences, the Dutch Cancer Society, the Cancer Genomics Centre, and the European Union under Marie Curie Actions (FP7). Work in M.P.'s laboratory is supported by grants from the NIH. M.P. is an investigator of the Howard Hughes Medical Institute. T.Y.L., S.M., and A.J.R.H. are supported by the Netherlands Proteomics Center. C.G.P. is funded by the Wellcome Trust. **Author contributions:** All authors designed the experiments and analyzed the data. F.K., L.Y., R.M., and R.L. performed most of the experiments. R.B. performed the in vitro ubiquitylation assays. R.M. and T.Y.L. performed the proteomic experiments. S.M. and A.J.R.H. supervised the proteomic studies. C.G.P. shared

unpublished data and provided reagents and technical support. M.P. contributed with initial funding, reagents, and suggestions. F.K. and D.G. wrote the manuscript. D.G. conceived and supervised the project. **Competing interests:** The authors declare that they have no competing interests. **Data and materials availability:** Scaffold files containing GeLC-MS/MS data can be downloaded from ProteomeCommons.org Tranche (https://proteomecommons.org/tranche) with the hash key and passphrase provided below. Hash: 7vUEg7l5ShPgDh6H-CaZBbNznpCi63nXCv/SCS5tWq1hc6pW8vNjDigrJ4pvDdzoUcbTBAFR+PXw5M49lh2-CUElxXnD0AAAAAAAAChg== Passphrase: NyCbEVxg1q3Mahvlh0JM.

Submitted 22 November 2011
Accepted 9 May 2012
Final Publication 5 June 2012
10.1126/scisignal.2002718
Citation: F. Kruiswijk, L. Yuniati, R. Magliozzi, T. Y. Low, R. Lim, R. Bolder, S. Mohammed, C. G. Proud, A. J. R. Heck, M. Pagano, D. Guardavaccaro, Coupled activation and degradation of eEF2K regulates protein synthesis in response to genotoxic stress. *Sci. Signal.* **5**, ra40 (2012).

Science Signaling

Coupled Activation and Degradation of eEF2K Regulates Protein Synthesis in Response to Genotoxic Stress

Flore Kruiswijk, Laurensia Yuniati, Roberto Magliozzi, Teck Yew Low, Ratna Lim, Renske Bolder, Shabaz Mohammed, Christopher G. Proud, Albert J. R. Heck, Michele Pagano and Daniele Guardavaccaro

Sci. Signal. **5** (227), ra40.
DOI: 10.1126/scisignal.2002718

Activated, Then Degraded, Stop-Start Regulation of Protein Synthesis

A key step in the process of translating mRNA into protein is the repositioning of the mRNA in the ribosome to enable elongation of the polypeptide chain. mRNA translocation in the ribosome is mediated by eukaryotic elongation factor 2 (eEF2), which is inhibited when phosphorylated by eEF2 kinase (eEF2K). Because protein synthesis is energetically costly, stressed cells inhibit this process to devote resources to stress responses. Kruiswijk *et al.* investigated the mechanisms by which genotoxic stress results in inhibition of protein synthesis. In response to a DNA-damaging agent, eEF2K was phosphorylated and activated by the kinase AMPK, thus leading to inhibition of eEF2 and a slowdown in elongation translation. eEF2K subsequently autophosphorylated itself in a motif recognized by the E3 ubiquitin ligase $SCF^{\beta TrCP}$, and the resulting degradation of eEF2K enabled elongation translation to resume. Thus, the activation and subsequent degradation of eEF2K by genotoxic stress are coupled to inhibition of protein synthesis in response to DNA damage and resumption of protein synthesis after DNA damage has been resolved.